

# Flat bands in Network Superstructures of Atomic Chains

Donghyeok Heo,<sup>1</sup> Jun Seop Lee,<sup>1</sup> Anwei Zhang,<sup>1,\*</sup> and Jun-Won Rhim<sup>1,2,†</sup>

<sup>1</sup>Department of Physics, Ajou University, Suwon 16499, Korea

<sup>2</sup>Research Center for Novel Epitaxial Quantum Architectures,

Department of Physics, Seoul National University, Seoul, 08826, Korea

We investigate the origin of the ubiquitous existence of flat bands in the network superstructures of atomic chains, where one-dimensional(1D) atomic chains array periodically. While there can be many ways to connect those chains, we consider two representative ways of linking them, the dot-type and triangle-type links. Then, we construct a variety of superstructures, such as the square, rectangular, and honeycomb network superstructures with dot-type links and the honeycomb superstructure with triangle-type links. These links provide the wavefunctions with an opportunity to have destructive interference, which stabilizes the compact localized state(CLS). The CLS is a localized eigenstate whose amplitudes are finite only inside a finite region and guarantees the existence of a flat band. In the network superstructures, there exist multiple flat bands proportional to the number of atoms of each chain, and the corresponding eigenenergies can be found from the stability condition of the compact localized state. Finally, we demonstrate that the finite bandwidth of the nearly flat bands of the network superstructures arising from the next-nearest-neighbor hopping processes can be suppressed by increasing the length of the chains consisting of the superstructures.

## I. INTRODUCTION

A flat band denotes a band with a zero group velocity over the whole Brillouin zone [1, 2]. When the flat band becomes slightly dispersive, which is the case in real experiments, we call it a nearly flat band [3]. The flat band systems have received great attention because of their intriguing many-body and geometric aspects. When the Coulomb interaction between electrons is introduced, the flat bands host unconventional superconductivity [4–12], ferromagnetism [13–19], Wigner crystal [20–23], and fractional Chern insulator [3, 24–33]. The quantum distance, one of the geometric quantities of the Bloch wavefunction, plays an important role in the anomalous Landau levels [34, 35], a new kind of bulk-interface correspondence [36], and appearance of the topological non-contractible loop states in flat band systems [37]. Moreover, it was revealed that the quantum metric [38] is the key quantity in the physics of the superfluidity [39, 40] and orbital magnetic susceptibility [41, 42].

Despite the numerous intriguing properties of the flat band, it has become a popular research subject only recently since the experimental realization of the nearly flat bands in the twisted bilayer graphene at the magic angle [5]. In addition to this, many artificial flat band systems have been examined [37, 43–49], lots of nearly flat band materials such as CoSn [50, 51] and FeSn [52] have been synthesized [53–57], and many candidate materials have been proposed theoretically recently [58–64]. We focus on the frequent appearance of flat bands in lattice structures with a large-size unit cell such as cyclic-graphyne, cyclic-graphdiyne, and honeycomb network in the nearly commensurate charge-density-wave phase of 1T-TaS<sub>2</sub> [17, 65]. Since these lattices are in the shape of a periodic network of finite-size 1D chains, they are called *network superstructures*. The common feature of network superstructures is that they host extremely flat bands at multiple

energy levels. Although the existence of the flat bands in several network superstructures such as those mentioned above was reported already [17, 65], the general understanding of why the flat bands are so ubiquitous in this class of systems and why there are multiple numbers of flat bands are developed is not studied yet.

In this paper, we understand the existence of flat bands in the network superstructures from the perspective of the special localized eigenmode of the flat band, so-called the compact localized state(CLS) [66–68]. The CLS is characterized by the fact that it has nonzero amplitude only inside a finite region in real space while exactly zero outside it. It was rigorously shown that one can always construct a CLS by a linear combination of the Bloch wave functions of a flat band [66]. If the Bloch wave function of the flat band does not have any singularity in momentum space, one can find  $N$  number of linearly independent CLSs to span the flat band completely, where  $N$  is the number of unit cells in the system. However, when the Bloch wave function becomes discontinuous due to a band-crossing with another band, the CLSs cannot form a complete set, and they are always linearly dependent. In this case, some non-compact eigenstates independent of the CLSs are required to exist to form a complete set of eigenfunctions spanning the flat band. Such non-compact states are usually found as non-contractible loop states(NLSs), which are extended along one spatial direction while compactly localized along another direction. NLSs show topological features in real space because they cannot be cut by adding CLSs and exhibit a winding feature over the whole system under the periodic boundary condition. This kind of flat band is called a *singular flat band*.

In the network superstructures, the CLS can be stabilized due to the destructive interference offered by the special lattice structure around the linking parts between 1D chains. We consider two representative types of the linking structure, the dot-type, and triangle-type. We construct various network superstructures by connecting the 1D chains in diverse ways and then show that they host many flat bands. The number of flat bands equals to the number of independent CLSs. While the

\* zawcuhk@gmail.com

† jwrhim@ajou.ac.kr

flat band becomes a nearly flat band when some long-range hopping processes are introduced, we show that the bandwidth of the nearly flat band can be suppressed by increasing the length of the 1D chains.

## II. NETWORK SUPERSTRUCTURES HOSTING FLAT BANDS

Since the existence of the flat band is equivalent to the presence of the CLS, we can obtain a flat band model by designing a lattice structure stabilizing the CLS. While the CLS has zero amplitudes outside a finite region, it should maintain the same shape after the hopping processes to be an eigenmode. To this end, destructive interference is necessary to avoid any dissipation of the amplitudes of the CLS after the hopping processes. As an example, the kagome lattice with the nearest-neighbor hopping processes can stabilize the hexagon-shaped CLS. In network superstructures, such destructive interference is expected to occur via the hopping processes at the lattice sites linking the neighboring 1D chains. In the following, we explain how this is possible in network superstructures.

Examples of the network superstructures are illustrated in FIG. 1(a), (e), and FIG. 2(a). First, the lattice structures in FIG. 1 are called network superstructures with dot-type links because the 1D chains are linked by purple-colored dots. The cyclicgraphyne and cyclicgraphdiyne belong to this category. Here, the 1D chain indicates the black dots in a straight line between two neighboring dot-type links. The sites in a 1D chain are labeled as the  $n$ -th dot in the  $m$ -th chain. The length of the  $m$ -th chain is represented by  $Q_m$ , which counts the number of sites in the  $m$ -th chain. If the length of all the chains is the same, it is simply described by  $Q$ . The amplitude of the CLS at the  $n$ -th dot in the  $m$ -th chain is denoted by  $a_{m,n}$ . On the other hand, the amplitude of the CLS vanishes at the links. The CLS can be stabilized in these lattice structures because the amplitudes at the neighboring sites of the dot-type link show destructive interference at the dot-type link after the hopping processes.

Second, the network structures in FIG. 2 are called network superstructures with triangle-type links because the 1D chains are linked by purple-colored triangular bonds. The charge-density-wave phase of 1T-TaS<sub>2</sub> belongs to this class. In this lattice structure, the amplitudes at the end sites of the neighboring 1D chains experience destructive interference via the triangular hopping structure. For example, the amplitudes  $a_{1,Q-1}$  and  $a_{2,0}$  of the first and second 1D chains will meet at another site in the triangle where they belong to and vanish after the hopping processes if  $a_{1,Q-1} = -a_{2,0}$ .

## III. TIGHT-BINDING ANALYSIS

### A. General recursion relation

The typical form of the CLSs of the network superstructures hosting flat bands is given by

$$|\chi\rangle = \sum_{m=1}^M \sum_{n=1}^{Q_m} a_{m,n} |m, n\rangle, \quad (1)$$

where  $a_{m,n}$  is the amplitude of the CLS at the  $n$ -th atom of the  $m$ -th chain. For the CLS to be an eigenstate of the given tight-binding Hamiltonian with the nearest-neighbor hopping parameter 1, the amplitudes should satisfy

$$a_{m,n} + a_{m,n-2} = \varepsilon a_{m,n-1}, \quad (2)$$

where  $\varepsilon$  is the energy of the flat band. Without loss of generality, one can assume that  $a_{m,0} = 1$  releasing the normalization condition for the CLS. Boundary conditions for the chain at two ends of it determine  $a_{m,1}$  and  $\varepsilon$ . Let us assume that we know the value of  $a_{m,1}$  from one of the boundary conditions. Then, the recursion relation (2) can be rewritten as

$$b_{m,n} = (\varepsilon - \alpha_\varepsilon) b_{m,n-1}, \quad (3)$$

where  $b_{m,n} = a_{m,n} - \alpha_\varepsilon a_{m,n-1}$ . Here,  $\alpha_\varepsilon$  satisfies  $\alpha_\varepsilon = 1/(\varepsilon - \alpha_\varepsilon)$ , namely,

$$\alpha_\varepsilon = \frac{\varepsilon \pm \sqrt{\varepsilon^2 - 4}}{2}. \quad (4)$$

From (3), we obtain

$$b_{m,n} = (\varepsilon - \alpha_\varepsilon)^{n-1} b_{m,1}, \quad (5)$$

which leads to

$$a_{m,n} = F_{n+1}(\alpha_\varepsilon) + (a_{m,1} - \varepsilon) F_n(\alpha_\varepsilon), \quad (6)$$

where

$$F_n(\alpha_\varepsilon) = \frac{\alpha_\varepsilon^n - \alpha_\varepsilon^{-n}}{\alpha_\varepsilon - \alpha_\varepsilon^{-1}}. \quad (7)$$

Since the eigenenergy of an infinite simple chain with the nearest-neighbor hopping parameter 1 lies between -2 and 2, it is reasonable to seek flat band energies in the same interval. Therefore, we can express the eigenenergy of the finite chain as  $\varepsilon = 2 \cos \theta$ , which leads to

$$\alpha_\varepsilon = e^{\pm i\theta}. \quad (8)$$

Note that  $\theta \neq 0$  to ensure the function  $F_n$  is well-defined. Then,  $F_n(\alpha_\varepsilon)$  is simplified as

$$F_n(\alpha_\varepsilon) = \frac{\sin n\theta}{\sin \theta}. \quad (9)$$

The explicit forms of the amplitudes of the CLS and the corresponding eigenenergy are determined from the boundary conditions of the chain at the links attached to it. The detailed forms of the eigenenergies of the flat bands of various network superstructures are derived in the following subsections.

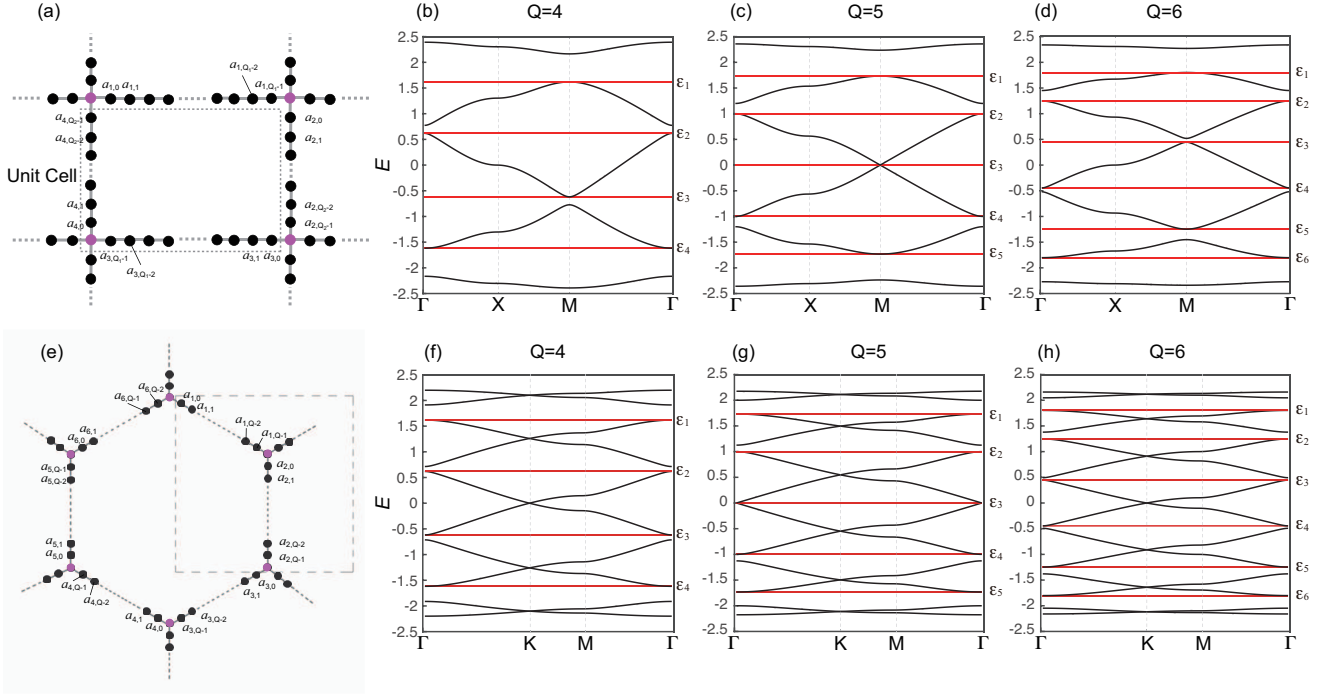


FIG. 1. (a) and (e) plot the rectangular and honeycomb network superstructures with dot-type links respectively. When  $Q_1 = Q_2$ , the rectangular network superstructure becomes the square network superstructure. Dot-type links are represented by purple color.  $a_{m,n}$  reads the amplitude of the CLS. In the network superstructures with dot-type links, the CLS's amplitude at the dot-type link is always zero. In the unit cell of the rectangular network, we have  $Q_1 + Q_2 + 1$  sites, while we have  $3Q + 2$  sites in the honeycomb case. From (b) to (d) and (f) to (h), we plot band structures of the square and honeycomb network superstructures with different sizes  $Q$ . Here, red lines represent the flat bands, whose energies are denoted by  $\epsilon_n$ . Here, only the nearest-neighbor hopping processes are considered.

## B. Network superstructures with dot-type links

We first consider a square network superstructure, which contains two simple chains of the same size in a unit cell as illustrated in FIG. 1(a) with  $Q_1 = Q_2$ . The simple chains are connected to each other by dot-type links. As shown in FIG. 1(a), we consider a CLS having zero amplitudes at the dot-type links. As a result, for the chain with  $m = 1$ , as an example, the recursion relation (2) for  $n = 1$  is given by

$$a_{1,1} = \epsilon a_{1,0} = \epsilon, \quad (10)$$

because  $a_{m,n}$  is assumed to be zero for a negative  $n$  and 1 for  $n = 0$ . By plugging-in this value of  $a_{1,1}$  into (6), the general term of the amplitude of the CLS along the  $m$ -th chain is obtained as

$$a_{1,n} = F_{n+1}(\alpha_\epsilon), \quad (11)$$

for  $0 \leq n \leq Q_1 - 1$ . When  $n = Q_1 - 1$ , namely at the end of the simple chain, the recursion relation (2) becomes

$$a_{1,Q_1-2} = \epsilon a_{1,Q_1-1}, \quad (12)$$

because  $a_{1,Q_1}$  is supposed to be zero. By applying (11) and  $\epsilon = 2 \cos \theta$  to the above, we obtain

$$2 \cos \theta \sin Q_1 \theta = \sin(Q_1 - 1) \theta, \quad (13)$$

which can be simplified into

$$\sin(Q_1 + 1) \theta = 0. \quad (14)$$

From the solution of (14),  $\theta = q\pi/(Q_1 + 1)$ , where  $q = 1, 2, \dots, Q_1$ , the eigenenergy of the flat band is evaluated as

$$\epsilon_q = 2 \cos \frac{q}{Q_1 + 1} \pi. \quad (15)$$

Note that  $q = 0$  and  $q = Q_1 + 1$  are excluded because the corresponding eigenenergy is 2 which makes  $\alpha_\epsilon = \pm 1$  and  $F_n$  ill-defined. Also, we only considered positive  $\theta$ 's because  $F_n(\alpha_\epsilon)$  is an even function of  $\theta$ , and we obtain the same CLS and eigenenergy for  $\theta$  and  $-\theta$ . By noting that  $a_{1,Q_1-1} = F_{Q_1}(\alpha_{\epsilon_q}) = (-1)^{q-1}$  for the flat band at  $\epsilon = \epsilon_q$ , the amplitudes of the CLS on other simple chains are given by  $a_{2,n} = (-1)^q a_{1,n}$ ,  $a_{3,n} = a_{1,n}$ ,  $a_{4,n} = (-1)^q a_{1,n}$ . Since all the simple chains have the same size,  $n$  runs from 0 to  $Q_1 - 1$  for all  $m$ . We confirmed that the formula (15) matches well with the flat band energies obtained numerically as shown in FIG. 1(b) to (d) for various values of  $Q$ .

The results of the eigenenergies and eigenfunctions of the CLSs in the above can be applied to any kind of network superstructures with dot-type links if the simple chains consisting of the network are of the same size. For example, the CLS of the honeycomb network superstructure is illustrated in FIG. 1(e), and the destructive interference at the dot-type links

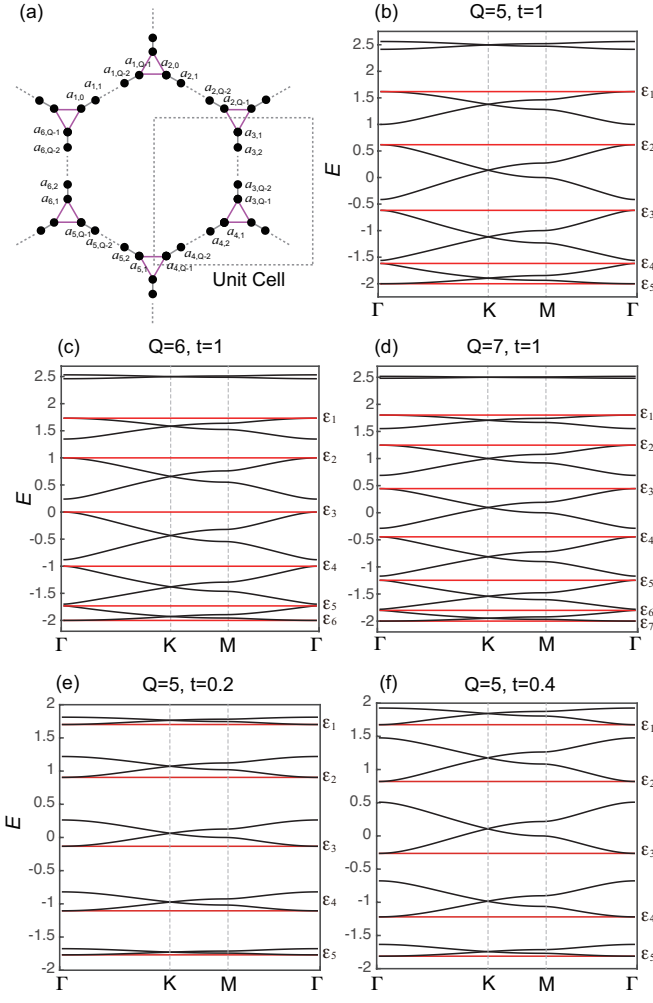


FIG. 2. (a) The honeycomb network superstructure with the triangle-type links. The triangle-type links are colored purple. In the unit cell, there are  $2Q$  sites. The hopping parameter for the triangle-type link is denoted by  $t$ , while it is 1 otherwise. From (b) to (d), we plot band spectra with  $t = 1$ , while we consider  $t \neq 1$  cases in (e) and (f). Flat bands are represented by red curves.

can be hosted by letting the amplitudes of the CLS satisfy  $a_{m,n} = (-1)^{m-1} a_{1,n}$ . The eigenenergies of the flat bands are completely described by (15). The tight-binding calculations of the band structures of the honeycomb network of superstructures are exhibited in FIG. 1(f) to (h).

One can have flat bands even if the network superstructure consists of simple chains of different sizes ( $Q_1 \neq Q_2$ ). Refer to the rectangular network superstructure illustrated in FIG. 1(a). The allowed eigenenergies of determined from these two chains are denoted by  $\varepsilon_q^{(1)} = 2 \cos q\pi / (Q_1 + 1)$  and  $\varepsilon_q^{(2)} = 2 \cos q\pi / (Q_2 + 1)$ . While the condition for the existence of a flat band is that the two chains share the same eigenenergy, there exist integers  $q_1$  and  $q_2$  that make  $\varepsilon_{q_1}^{(1)} = \varepsilon_{q_2}^{(2)}$  if  $Q_1 + 1$  and  $Q_2 + 1$  have a common divisor larger than 1 and smaller than  $\min(Q_1 + 1, Q_2 + 1)$ . In FIG. 3, we plot various examples of rectangular network superstructures

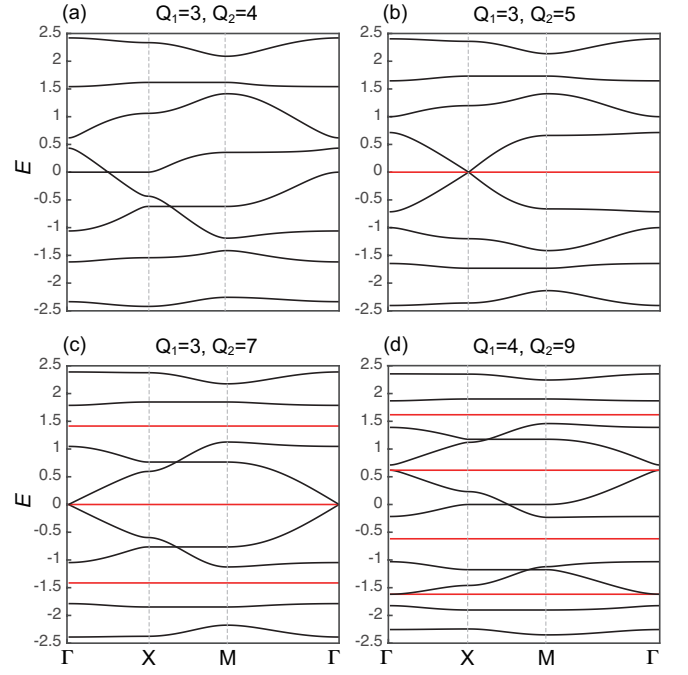


FIG. 3. (a) Band spectra of rectangular network superstructures with  $Q_1 \neq Q_2$ . Red lines denote flat bands. Refer to FIG. 1(a) for the lattice structure.

with dot-type links. As shown in FIG. 3(a), one cannot have a flat band because  $Q_1 + 1 = 4$  and  $Q_2 + 1 = 5$  have no common divisor. On the other hand, if  $Q_1 = 3$  and  $Q_2 = 5$ , one can have a flat band when  $q_1 = 2$  and  $q_2 = 3$  as illustrated in FIG. 3(b). If  $Q_2 + 1$  is an integer multiple of  $Q_1 + 1$ , we have  $Q_1$  number of flat bands as plotted in FIG. 3(c) and (d).

### C. Network superstructures with triangle-type links

The triangle-type links are illustrated in FIG. 2(a). Unlike dot-type links, triangle-type links let the simple chains connect to each other directly. Let us consider the honeycomb network consisting of simple chains of the same size  $Q$ . We solve the recursion equation (2) for the  $m = 1$  simple chain, which neighbors with the  $m = 2$  and  $m = 6$  chains. Assuming  $a_{1,0} = 1$ , one can note that we should have  $a_{6,Q-1} = -1$  to prevent the dissipation of the CLS via the destructive interference at the triangle-type link. Then, the recursion relation relevant to the amplitudes of the CLS at the link sites is given by

$$a_{1,1} + a_{6,Q-1} = a_{1,1} - 1 = \varepsilon a_{1,0} = \varepsilon, \quad (16)$$

which gives  $a_{1,1} = \varepsilon + 1$ . From (6), the general term of the amplitude of the CLS on the  $m = 1$  simple chain is obtain as

$$a_{1,n} = F_{n+1}(\alpha_\varepsilon) + F_n(\alpha_\varepsilon), \quad (17)$$

$$= \frac{\sin(n+1)\theta + \sin n\theta}{\sin \theta}. \quad (18)$$

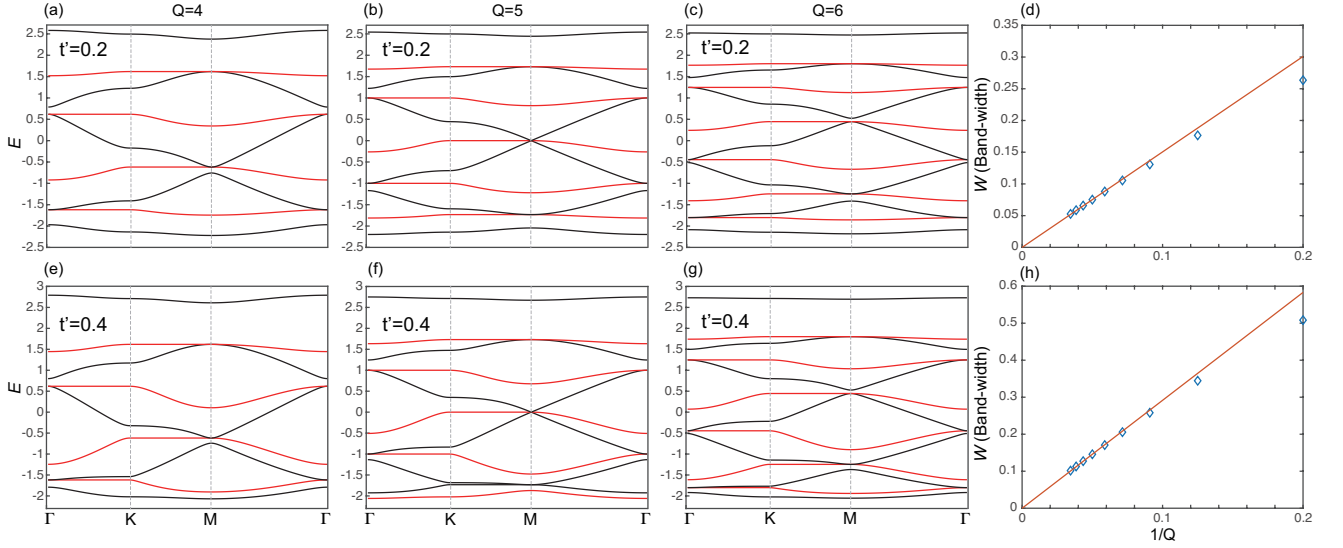


FIG. 4. Band structures of the square network superstructures with the next nearest-neighbor hopping processes ( $t'$ ) between four sites around the dot-type link in FIG. 1(a). The flat bands in FIG. 1(b) to (d) deform to the nearly flat bands colored red in (a) to (c) and (e) to (g) for  $t' = 0.2$  and  $0.4$ , respectively. In (d) and (h), we plot the bandwidth of the nearly flat band as a function of  $1/Q$ . Here, we take the maximum bandwidth among all the nearly flat bands for a given  $Q$ .

Due to the destructive interference at the other triangle link involving  $a_{1,Q-1}$  and  $a_{2,0}$ , we have  $a_{2,0} = -a_{1,Q-1}$ , which results in  $a_{2,n} = -a_{1,Q-1}[F_{n+1}(\alpha_\varepsilon) + F_n(\alpha_\varepsilon)] = -a_{1,Q-1}a_{1,n}$ . This means that  $a_{2,Q-1} = -a_{1,Q-1}^2$ . By applying the same process to the other chains, we obtain  $a_{6,Q-1} = -a_{1,Q-1}^6 = -1$ , which implies that  $a_{1,Q-1} = \pm 1$  because the function  $F_n(\alpha_\varepsilon)$  is real-valued. Then, the eigenvalue condition is given by

$$\sin Q\theta + \sin(Q-1)\theta = \pm \sin \theta, \quad (19)$$

which leads to  $\sin Q\theta/2 \times \cos(Q-1)\theta/2 = 0$  or  $\cos Q\theta/2 \times \sin(Q-1)\theta/2 = 0$ . On the other hand, the eigenvalue equation at another boundary of the  $m = 1$  chain is given by

$$a_{1,Q-2} + a_{2,0} = a_{1,Q-2} - a_{1,Q-1} = \varepsilon a_{1,Q-1}. \quad (20)$$

Here,  $a_{2,0} = a_{1,Q-1}$  to have destructive interference at the triangular link. By using the identity  $\varepsilon + 1 = a_{1,1}$  and the formula (18), we have another condition for  $\theta$  given by  $\sin Q\theta = 0$ . These conditions for  $\theta$  lead to the solutions of the form  $\theta = \pi q/Q$ , where  $q$  is an integer running from 1 to  $Q$ . Here,  $q = 0$  is excluded because this makes  $F_n(\alpha_\varepsilon)$  ill-defined as explained in Sec. III A. These solutions of  $\theta$  lead to the flat band energies given by

$$\varepsilon_q = 2 \cos \frac{\pi q}{Q}, \quad (21)$$

by putting these  $\theta$ 's into  $\varepsilon = 2 \cos \theta$  derived in Sec. III A.

#### D. Triangle-type link with different hopping amplitudes

The hopping parameters of the bonds in the triangle link can be different from 1, the hopping parameter of the simple

chains, as shown in Fig. . Let us denote the hopping parameter in the link by  $t$ . As in the previous cases, we set  $a_{1,0} = 1$ . Then, the recursion relation for determining  $a_{1,1}$  is given by

$$a_{1,1} + ta_{6,Q-1} = a_{1,1} - t = \varepsilon a_{1,0} = \varepsilon, \quad (22)$$

which results in  $a_{1,1} = \varepsilon + t$ . From, (6), the general term is evaluated as

$$a_{1,n} = F_{n+1}(\alpha_\varepsilon) + tF_n(\alpha_\varepsilon), \quad (23)$$

$$= \frac{\sin(n+1)\theta + t \sin n\theta}{\sin \theta}. \quad (24)$$

Eigenenergies of the flat bands are obtained from the condition  $a_{1,Q-1} = \pm 1$ , which leads to

$$\sin Q\theta + t \sin(Q-1)\theta \pm \sin \theta = 0. \quad (25)$$

Another boundary condition given by

$$a_{1,Q-2} + ta_{2,0} = a_{1,Q-2} - ta_{2,0} = \varepsilon a_{1,Q-1}, \quad (26)$$

gives

$$\sin(Q-1)\theta + t \sin(Q-2)\theta \pm (\sin 2\theta + t \sin \theta) = 0, \quad (27)$$

where the sign  $\pm$  is synchronized with that of (25). By solving the coupled equations (25) and (27) with the same sign, we obtain the flat band energies  $\varepsilon = 2 \cos \theta$ .

#### E. Effect of the next-nearest-neighbor hopping processes

Around the dot-type link in FIG. 1(a) and 1(e), let us consider the effect of the small next-nearest-neighbor hopping

processes. The corresponding parameter is denoted by  $t'$ . For example, in FIG. 1(a), the hopping processes between  $(m, n) = (1, 0)$  and  $(m, n) = (4, Q-1)$ ,  $(m, n) = (1, Q-1)$  and  $(m, n) = (2, 0)$ ,  $(m, n) = (2, Q-1)$  and  $(m, n) = (3, 0)$ , and  $(m, n) = (3, Q-1)$  and  $(m, n) = (4, 0)$  are the next-nearest-neighbor ones. As in many flat band models, the flat bands in the network superstructures are also easily warped when we include such long-range hopping interactions. We obtain band dispersions of the square network superstructures with  $t' = 0.2$  and  $0.4$  as exhibited in FIG. 4. The perfectly flat bands of the square network superstructures in FIG. 1 represented by red lines, deform to the nearly flat bands, also colored red, in FIG. 4. We noted in FIG. 4(d) and (h) that the bandwidth of the nearly flat bands decreases as  $1/Q$ . While the bandwidth of the nearly flat band scales with the effective hopping integral between localized modes at two neighboring 1D chains, the amplitudes at each site, such as  $a_{1,0}$  and  $a_{6,Q-1}$  are proportional to  $1/\sqrt{Q}$ . As a result, the bandwidth is proportional to  $t'/Q$ . These results imply that one can flatten the nearly flat band as much as one wants by increasing the length of the 1D chains consisting of the network superstructures.

#### IV. CONCLUSIONS

We have investigated the origin of the development of flat bands in network superstructures from the perspective of the stabilization of the CLSs because there is a correspondence

between the flat band. Two types of the bonding structures linking 1D chains offer the destructive interference, so that the CLSs satisfy the eigenstate condition. We have considered two types of links between 1D chains called dot-type and triangle-type links. By using these links, we have constructed the square, rectangular, and honeycomb network superstructures and obtained analytic forms of the flat band energies and CLSs. Note that the number of flat bands equals to the number of independent CLSs. While the previously studied network superstructures such as cyclic-graphyne, cyclic-graphdiyne, and honeycomb network in the nearly commensurate charge-density-wave phase of 1T-TaS<sub>2</sub> exhibit almost flat bands in spite of the long-range hopping processes, we demonstrated that this is because the overlap between localized modes in 1D chains scales as the inverse of the length of the chains. Therefore, one can flatten the nearly flat band as much as we want by increasing the length of the 1D chains.

#### Acknowledgements

D.H, J.S.L, A.Z. and J.-W.R. were supported by the National Research Foundation of Korea (NRF) Grant funded by the Korea government (MSIT) (Grant No. 2021R1A2C1010572). J.-W.R. was supported by the National Research Foundation of Korea (NRF) Grant funded by the Korea government (MSIT) (Grant No. 2021R1A5A1032996).

- 
- [1] D. Leykam, A. Andreanov, and S. Flach, Artificial flat band systems: from lattice models to experiments, *Advances in Physics: X* **3**, 1473052 (2018).
  - [2] J.-W. Rhim and B.-J. Yang, Singular flat bands, *Advances in Physics: X* **6**, 1901606 (2021).
  - [3] F. Wang and Y. Ran, Nearly flat band with chern number  $c=2$  on the dice lattice, *Physical Review B* **84**, 241103 (2011).
  - [4] G. Volovik, The fermi condensate near the saddle point and in the vortex core, *JETP Letters* **59**, 830 (1994).
  - [5] Y. Cao, V. Fatemi, S. Fang, K. Watanabe, T. Taniguchi, E. Kaxiras, and P. Jarillo-Herrero, Unconventional superconductivity in magic-angle graphene superlattices, *Nature* **556**, 43 (2018).
  - [6] X. Liu, C.-L. Chiu, J. Y. Lee, G. Farahi, K. Watanabe, T. Taniguchi, A. Vishwanath, and A. Yazdani, Spectroscopy of a tunable moiré system with a correlated and topological flat band, *Nature communications* **12**, 1 (2021).
  - [7] L. Balents, C. R. Dean, D. K. Efetov, and A. F. Young, Superconductivity and strong correlations in moiré flat bands, *Nature Physics* **16**, 725 (2020).
  - [8] V. Peri, Z.-D. Song, B. A. Bernevig, and S. D. Huber, Fragile topology and flat-band superconductivity in the strong-coupling regime, *Physical review letters* **126**, 027002 (2021).
  - [9] D. Yudin, D. Hirschmeier, H. Hafermann, O. Eriksson, A. I. Lichtenstein, and M. I. Katsnelson, Fermi condensation near van hove singularities within the hubbard model on the triangular lattice, *Physical Review Letters* **112**, 070403 (2014).
  - [10] G. E. Volovik, Graphite, graphene, and the flat band superconductivity, *JETP Letters* **107**, 516 (2018).
  - [11] H. Aoki, Theoretical possibilities for flat band superconductivity, *Journal of Superconductivity and Novel Magnetism* **33**, 2341 (2020).
  - [12] A. Kononov, M. Endres, G. Abulizi, K. Qu, J. Yan, D. G. Mandrus, K. Watanabe, T. Taniguchi, and C. Schönerberger, Superconductivity in type-ii weyl-semimetal wte2 induced by a normal metal contact, *Journal of Applied Physics* **129**, 113903 (2021).
  - [13] A. Mielke, Ferromagnetism in the hubbard model and hund's rule, *Physics Letters A* **174**, 443 (1993).
  - [14] H. Tasaki, From nagaoka's ferromagnetism to flat-band ferromagnetism and beyond: an introduction to ferromagnetism in the hubbard model, *Progress of theoretical physics* **99**, 489 (1998).
  - [15] A. Mielke, Stability of ferromagnetism in hubbard models with degenerate single-particle ground states, *Journal of Physics A: Mathematical and General* **32**, 8411 (1999).
  - [16] I. Hase, T. Yanagisawa, Y. Aiura, and K. Kawashima, Possibility of flat-band ferromagnetism in hole-doped pyrochlore oxides  $sn\ 2\ o\ 7$  and  $sn\ 2\ ta\ 2\ o\ 7$ , *Physical review letters* **120**, 196401 (2018).
  - [17] J.-Y. You, B. Gu, and G. Su, Flat band and hole-induced ferromagnetism in a novel carbon monolayer, *Scientific reports* **9**, 1 (2019).
  - [18] Y. Saito, J. Ge, L. Rademaker, K. Watanabe, T. Taniguchi, D. A. Abanin, and A. F. Young, Hofstadter subband ferromagnetism and symmetry-broken chern insulators in twisted bilayer graphene, *Nature Physics* **17**, 478 (2021).

- [19] A. L. Sharpe, E. J. Fox, A. W. Barnard, J. Finney, K. Watanabe, T. Taniguchi, M. Kastner, and D. Goldhaber-Gordon, Emergent ferromagnetism near three-quarters filling in twisted bilayer graphene, *Science* **365**, 605 (2019).
- [20] C. Wu, D. Bergman, L. Balents, and S. D. Sarma, Flat bands and wigner crystallization in the honeycomb optical lattice, *Physical review letters* **99**, 070401 (2007).
- [21] Y. Chen, S. Xu, Y. Xie, C. Zhong, C. Wu, and S. Zhang, Ferromagnetism and wigner crystallization in kagome graphene and related structures, *Physical Review B* **98**, 035135 (2018).
- [22] B. Jaworowski, A. D. Güçlü, P. Kaczmarkiewicz, M. Kupczyński, P. Potasz, and A. Wójs, Wigner crystallization in topological flat bands, *New Journal of Physics* **20**, 063023 (2018).
- [23] J.-W. Rhim, J. K. Jain, and K. Park, Analytical theory of strongly correlated wigner crystals in the lowest landau level, *Physical Review B* **92**, 121103 (2015).
- [24] E. Tang, J.-W. Mei, and X.-G. Wen, High-temperature fractional quantum hall states, *Physical review letters* **106**, 236802 (2011).
- [25] K. Sun, Z. Gu, H. Katsura, and S. D. Sarma, Nearly flatbands with nontrivial topology, *Physical review letters* **106**, 236803 (2011).
- [26] T. Neupert, L. Santos, C. Chamon, and C. Mudry, Fractional quantum hall states at zero magnetic field, *Physical review letters* **106**, 236804 (2011).
- [27] D. Sheng, Z.-C. Gu, K. Sun, and L. Sheng, Fractional quantum hall effect in the absence of landau levels, *Nature communications* **2**, 1 (2011).
- [28] N. Regnault and B. A. Bernevig, Fractional chern insulator, *Physical Review X* **1**, 021014 (2011).
- [29] C. Weeks and M. Franz, Flat bands with nontrivial topology in three dimensions, *Physical Review B* **85**, 041104 (2012).
- [30] M. Trescher and E. J. Bergholtz, Flat bands with higher chern number in pyrochlore slabs, *Physical Review B* **86**, 241111 (2012).
- [31] S. Yang, Z.-C. Gu, K. Sun, and S. D. Sarma, Topological flat band models with arbitrary chern numbers, *Physical Review B* **86**, 241112 (2012).
- [32] Z. Liu, E. J. Bergholtz, H. Fan, and A. M. Läuchli, Fractional chern insulators in topological flat bands with higher chern number, *Physical review letters* **109**, 186805 (2012).
- [33] E. J. Bergholtz and Z. Liu, Topological flat band models and fractional chern insulators, *International Journal of Modern Physics B* **27**, 1330017 (2013).
- [34] J.-W. Rhim, K. Kim, and B.-J. Yang, Quantum distance and anomalous landau levels of flat bands, *Nature* **584**, 59 (2020).
- [35] Y. Hwang, J.-W. Rhim, and B.-J. Yang, Geometric characterization of anomalous landau levels of isolated flat bands, *Nature communications* **12**, 1 (2021).
- [36] C.-g. Oh, D. Cho, S. Y. Park, and J.-W. Rhim, Bulk-interface correspondence from quantum distance in flat band systems, *arXiv preprint arXiv:2203.14576* (2022).
- [37] J. Ma, J.-W. Rhim, L. Tang, S. Xia, H. Wang, X. Zheng, S. Xia, D. Song, Y. Hu, Y. Li, *et al.*, Direct observation of flatband loop states arising from nontrivial real-space topology, *Physical Review Letters* **124**, 183901 (2020).
- [38] Y. Hwang, J. Jung, J.-W. Rhim, and B.-J. Yang, Wave-function geometry of band crossing points in two dimensions, *Physical Review B* **103**, L241102 (2021).
- [39] S. Peotta and P. Törmä, Superfluidity in topologically nontrivial flat bands, *Nature communications* **6**, 1 (2015).
- [40] A. Julku, S. Peotta, T. I. Vanhala, D.-H. Kim, and P. Törmä, Geometric origin of superfluidity in the lieb-lattice flat band, *Physical review letters* **117**, 045303 (2016).
- [41] A. Raoux, F. Piéchon, J.-N. Fuchs, and G. Montambaux, Orbital magnetism in coupled-bands models, *Physical Review B* **91**, 085120 (2015).
- [42] F. Piéchon, A. Raoux, J.-N. Fuchs, and G. Montambaux, Geometric orbital susceptibility: Quantum metric without berry curvature, *Physical Review B* **94**, 134423 (2016).
- [43] D. Guzmán-Silva, C. Mejía-Cortés, M. Bandres, M. Rechtsman, S. Weimann, S. Nolte, M. Segev, A. Szameit, and R. Vicencio, Experimental observation of bulk and edge transport in photonic lieb lattices, *New Journal of Physics* **16**, 063061 (2014).
- [44] R. A. Vicencio, C. Cantillano, L. Morales-Inostroza, B. Real, C. Mejía-Cortés, S. Weimann, A. Szameit, and M. I. Molina, Observation of localized states in lieb photonic lattices, *Physical review letters* **114**, 245503 (2015).
- [45] S. Mukherjee, A. Spracklen, D. Choudhury, N. Goldman, P. Öhberg, E. Andersson, and R. R. Thomson, Observation of a localized flat-band state in a photonic lieb lattice, *Physical review letters* **114**, 245504 (2015).
- [46] S. Xia, A. Ramachandran, S. Xia, D. Li, X. Liu, L. Tang, Y. Hu, D. Song, J. Xu, D. Leykam, *et al.*, Unconventional flatband line states in photonic lieb lattices, *Physical review letters* **121**, 263902 (2018).
- [47] D. Leykam and S. Flach, Perspective: photonic flatbands, *Apl Photonics* **3**, 070901 (2018).
- [48] Y. Xie, L. Song, W. Yan, S. Xia, L. Tang, D. Song, J.-W. Rhim, and Z. Chen, Fractal-like photonic lattices and localized states arising from singular and nonsingular flatbands, *APL Photonics* **6**, 116104 (2021).
- [49] L. Song, Y. Xie, S. Xia, L. Tang, D. Song, J.-W. Rhim, and Z. Chen, Topological flatband loop states in fractal-like photonic lattices, *arXiv preprint arXiv:2204.13899* (2022).
- [50] M. Kang, S. Fang, L. Ye, H. C. Po, J. Denlinger, C. Jozwiak, A. Bostwick, E. Rotenberg, E. Kaxiras, J. G. Checkelsky, *et al.*, Topological flat bands in frustrated kagome lattice cosn, *Nature communications* **11**, 1 (2020).
- [51] Z. Liu, M. Li, Q. Wang, G. Wang, C. Wen, K. Jiang, X. Lu, S. Yan, Y. Huang, D. Shen, *et al.*, Orbital-selective dirac fermions and extremely flat bands in frustrated kagome-lattice metal cosn, *Nature communications* **11**, 1 (2020).
- [52] M. Kang, L. Ye, S. Fang, J.-S. You, A. Levitan, M. Han, J. I. Facio, C. Jozwiak, A. Bostwick, E. Rotenberg, *et al.*, Dirac fermions and flat bands in the ideal kagome metal fesn, *Nature materials* **19**, 163 (2020).
- [53] J.-X. Yin, S. S. Zhang, G. Chang, Q. Wang, S. S. Tsirkin, Z. Guguchia, B. Lian, H. Zhou, K. Jiang, I. Belopolski, *et al.*, Negative flat band magnetism in a spin-orbit-coupled correlated kagome magnet, *Nature Physics* **15**, 443 (2019).
- [54] L. Ye, M. Kang, J. Liu, F. Von Cube, C. R. Wicker, T. Suzuki, C. Jozwiak, A. Bostwick, E. Rotenberg, D. C. Bell, *et al.*, Massive dirac fermions in a ferromagnetic kagome metal, *Nature* **555**, 638 (2018).
- [55] Z. Lin, J.-H. Choi, Q. Zhang, W. Qin, S. Yi, P. Wang, L. Li, Y. Wang, H. Zhang, Z. Sun, *et al.*, Flatbands and emergent ferromagnetic ordering in fe 3 sn 2 kagome lattices, *Physical review letters* **121**, 096401 (2018).
- [56] T. Yang, Q. Wan, Y. Wang, M. Song, J. Tang, Z. Wang, H. Lv, N. Plumb, M. Radovic, G. Wang, *et al.*, Evidence of orbit-selective electronic kagome lattice with planar flat-band in correlated paramagnetic ycr6ge6, *arXiv preprint arXiv:1906.07140* (2019).
- [57] P. Wang, Y. Wang, B. Zhang, Y. Li, S. Wang, Y. Wu, H. Zhu, Y. Liu, G. Zhang, D. Liu, *et al.*, Experimental observation of

- electronic structures of kagome metal  $\text{YCrGe}_6$ , *Chinese Physics Letters* **37**, 087102 (2020).
- [58] I. Hase, T. Yanagisawa, and K. Kawashima, Flat-band in pyrochlore oxides: a first-principles study, *Nanomaterials* **9**, 876 (2019).
- [59] A. Skurativska, S. S. Tsirkin, F. D. Natterer, T. Neupert, and M. H. Fischer, Flat bands with fragile topology through superlattice engineering on single-layer graphene, *Physical Review Research* **3**, L032003 (2021).
- [60] M. S. de Sousa, F. Liu, F. Qu, and W. Chen, Vacancy-engineered flat-band superconductivity in holey graphene, *Physical Review B* **105**, 014511 (2022).
- [61] C. Xiao, A. Mostofi, and N. Bristowe, Flat band magnetism in electride monolayer  $\text{LaBr}_3$ , in *APS March Meeting Abstracts*, Vol. 2021 (2021) pp. A57–013.
- [62] D. M. Kennes, L. Xian, M. Claassen, and A. Rubio, One-dimensional flat bands in twisted bilayer germanium selenide, *Nature communications* **11**, 1 (2020).
- [63] M. G. Yamada, T. Soejima, N. Tsuji, D. Hirai, M. Dincă, and H. Aoki, First-principles design of a half-filled flat band of the kagome lattice in two-dimensional metal-organic frameworks, *Physical Review B* **94**, 081102 (2016).
- [64] N. Regnault, Y. Xu, M.-R. Li, D.-S. Ma, M. Jovanovic, A. Yazdani, S. S. Parkin, C. Felser, L. M. Schoop, N. P. Ong, *et al.*, Catalogue of flat-band stoichiometric materials, *Nature* **603**, 824 (2022).
- [65] J. M. Lee, C. Geng, J. W. Park, M. Oshikawa, S.-S. Lee, H. W. Yeom, and G. Y. Cho, Stable flatbands, topology, and superconductivity of magic honeycomb networks, *Physical Review Letters* **124**, 137002 (2020).
- [66] J.-W. Rhim and B.-J. Yang, Classification of flat bands according to the band-crossing singularity of Bloch wave functions, *Physical Review B* **99**, 045107 (2019).
- [67] Y. Hwang, J.-W. Rhim, and B.-J. Yang, Flat bands with band crossings enforced by symmetry representation, *Physical Review B* **104**, L081104 (2021).
- [68] Y. Hwang, J.-W. Rhim, and B.-J. Yang, General construction of flat bands with and without band crossings based on wave function singularity, *Physical Review B* **104**, 085144 (2021).